Chemical Engineering Science 60 (2005) 4397–4407

Chemical Engineering Science

www.elsevier.com/locate/ces

Separation of carbon dioxide and methane in continuous countercurrent gas centrifuges

Ralph van Wissen[a], Michael Golombok[b], J.J.H. Brouwers[a,*]

[a]*Department of Mechanical Engineering, Den Dolech 2, TU Eindhoven, 5600 MB Eindhoven, The Netherlands*
[b]*Shell International Exploration and Production, Kessler Park 1, 2288 GS Rijswijk, The Netherlands*

Received 19 November 2004; received in revised form 1 March 2005; accepted 3 March 2005
Available online 3 May 2005

Abstract

The goal of this study is to determine the order of magnitude of the maximum achievable separation for decontaminating a natural gas well using a gas centrifuge. Previously established analytical approximations are not applicable for natural gas decontamination. Numerical simulations based on the batch case show that although the separative strength of the centrifuge is quite good, its throughput is very limited. Both enrichment and throughput are only a function of length and peripheral velocity. A centrifuge with a length of 5 m and a peripheral velocity of approximately 800 m/s would have a throughput of 0.57 mol/s and a product flow of 0.17 mol/s. These numbers are calculated with the assumption that the centrifuge is refilled and spun up instantaneously. The results for the countercurrent centrifuge show how the production rate varies as a function of internal circulation, product–feed ratio, peripheral velocity and centrifuge length and radius. Under conditions similar to those of the batch case the production is approximately half compared to the batch case, i.e., 0.08 mol/s. Optimization can yield a higher production at the cost of lower enrichment. Considering the current natural gas prices and the low production rate of the centrifuge, it is certain that the gas centrifuge will not generate enough revenue to make up for the high investment costs.

Keywords: Carbon dioxide; Methane; Gas centrifuge

1. Introduction

A large part of the world's natural gas reserves that have been discovered to date are currently not available for production due to limitations in separation technology. These gas fields contain large amounts of contaminating gases, mainly CO_2 and also H_2S (Golombok and Morley, 2004). By large amounts we mean $> 10\%$ CO_2 and $> 1\%$ H_2S. At lower levels of contamination, amine treatment is currently used for removing CO_2 and H_2S from well gas (Kohl and Nielsen, 1997). This process uses large amounts of energy even for low contaminations; the reheater that is required to recycle the absorption fluid is the main cost. A second disadvantage is that the waste gases are produced at atmospheric pressure, which results in high compression costs for reinjection. Due to these two disadvantages it is currently too expensive to produce from gas fields that contain more than 5–10% CO_2 and 1% H_2S.

A limited number of papers have previously examined the application of gas centrifuges to gas separation outside the usual isotope enrichment area of interest (Auvil and Wilkinson, 1972; Williams, 1980; Golombok and Chewter, 2004; Cracknell and Golombok, 2004). This technique does not have the disadvantages of the amine process; however, there are some other difficulties which prevent direct implementation. One is the secrecy surrounding centrifuges. Though understandable because centrifuges are commonly used to produce highly enriched uranium, it means that there are few publications by people who have actually worked with them (Beams and Skarstrom, 1939; Groth and Beyerle, 1961; Los, 1963; Brouwers, 1976, 1978a,b). Literature on the application of the gas centrifuge for non-isotopic separation is scarce whereas natural gas separation by membranes and solvent absorption is well established (Astarita et al., 1983;

* Corresponding author. Tel.: +31 40 2475397.
E-mail address: j.j.h.brouwers@tue.nl (J.J.H. Brouwers).

0009-2509/$ - see front matter © 2005 Elsevier Ltd. All rights reserved.
doi:10.1016/j.ces.2005.03.010

Kohl and Nielsen, 1997; Maddox and Morgan, 1998). A second disadvantage of the centrifuge is its high rotational speed which is essential for the process, but also requires very advanced technologies.

In Section 2, we briefly overview the batch centrifuge as a basis from which the more complicated continuous countercurrent model can be developed. Practical operation requires a continuous device; however previously developed results and derivations are not fully applicable due to several fundamental differences between isotope separation and CH_4–CO_2 separation which we formulate and develop in Section 3. A similar approach to obtain a simplified differential equation for the countercurrent centrifuge is infeasible because we are dealing with matter with large differential molecular weight in contrast to uranium isotopes where the difference in molecular weight is relatively small. Therefore in order to assess achievable flows and separation in this paper the convection–diffusion equation is solved numerically. The same numerical code is also used to determine the influence of design parameters—the results are described in Section 4.

2. Batch centrifuge

A gas centrifuge is basically a rotating hollow cylinder which is filled with a gas mixture. Batch centrifugation is not very interesting for industrial application; however, because of the conceptual simplicity it is very useful for getting a better understanding of the basic working principle and for examining the influence of parameters such as pressure, speed and temperature.

The operating characteristics of the gas–gas batch centrifuge have been extensively reviewed in previous reports along with the modifications we have introduced for the application to natural gas (Golombok and Chewter, 2004). A brief summary is given here in order to place the process development in a general context. The gas centrifuge is easiest understood by reference to Fig. 1. A mass of gas with two components of different molecular weight is spun up. A pressure gradient develops nearly instantaneously with a concentration gradient for each component. Diffusion occurs along this concentration gradient until the centrifugal force is balanced.

Large centrifugal forces push the gas to the wall, resulting in a pressure gradient which for a steady-state batch centrifuge is described for each component i by (Auvil and Wilkinson, 1976)

$$p_i(r) = p_i(0)\mathrm{e}^{A_i r^2}, \tag{1}$$

where p_i is partial pressure of component i (MPa) and r is the radial coordinate (m). The coefficient A_i is defined by

$$A_i = \frac{M_i \Omega^2}{2R_g T}, \tag{2}$$

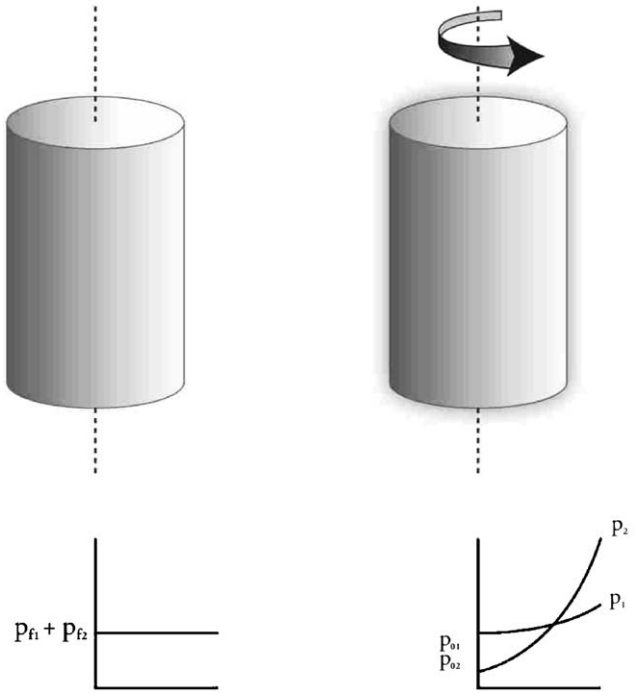

Fig. 1. Schematic of batch centrifuge showing pressure distribution of two components under feed conditions and following spin-up.

where M_i is the molecular weight of component i, Ω is the angular velocity, R_g the gas constant and T the temperature. Note that Eq. (1) assumes ideal gas behaviour. In fact at higher pressures near the rotor periphery, dewpointing will occur and the model we have described would be inadequate for predicting the formation of condensation. We have previously shown that condensation can be described quantitatively (Cracknell and Golombok, 2004) using a statistically based molecular interaction model. Based on these equations, gases with different molecular weights have different partial pressure profiles; therefore in steady-state operation their mole fraction profiles vary with radius. Cohen derived the partial differential equation which describes the time-dependent mole fraction distribution in a gas centrifuge of any type (Cohen, 1951). The simplified equation for a gas mixture consisting of two components denoted with subscripts 1 and 2 is

$$\rho \frac{\partial x_1}{\partial t} + \rho v_z \frac{\partial x_1}{\partial z} + \rho v_r \frac{\partial x_1}{\partial r} = \frac{\rho D}{r} \frac{\partial}{\partial r}\left(r \frac{\partial x_1}{\partial r} + 2A x_1 (1 - x_1) r^2 \right) + \rho D \frac{\partial^2 x_1}{\partial z^2}, \tag{3}$$

where D is the diffusion coefficient (m^2/s), ρ the mixture mass density ($kmol/m^3$), z the axial coordinate (m), t the time (s), v_i the gas mixture velocity in direction i (m/s), x_1

the mole fraction of component A where (Pratt, 1967)

$$A = A_2 - A_1 \quad (2a).$$

Here, the terms on the left-hand side represent change of mass transport per unit volume by instationarity and by convection. These changes are balanced by diffusion represented by the r.h.s. The following assumptions were made during the derivation of this equation:

- ρD is a constant.
- Temperature is constant throughout the gas, i.e., $T = T_0$.
- Convective velocities of both components are assumed to be the same.

For a better understanding of the influence of the design parameters length and radius and to simplify the numerical modelling, the following dimensionless coordinates are introduced: $z^* = z/l_0$ and $r^* = r/r_0$, where l_0 is the centrifuge length (m) and r_0 the centrifuge radius (m). For a batch centrifuge with no internal convection, Eq. (2) can be simplified to

$$\frac{\rho r_0^2}{\rho D}\frac{\partial x_1}{\partial t} = \frac{1}{r^*}\frac{\partial}{\partial r^*}\left(r^*\frac{\partial x_1}{\partial r^*} + 2Ar_0^2 x_1(1-x_1)r^{*2}\right). \quad (4)$$

Since there is no axial flow in the batch centrifuge, terms in $\partial/\partial z$ are neglected. Thus the mole fraction is independent of the axial coordinate $x_1 \neq x_1(z)$. The right-hand side of this equation scales with $A_0 = Ar_0^2 = \Delta M v_0^2/(2RT)$, which is mainly dependent on the design parameter peripheral velocity, $v_0 = \Omega r_0$. From the left-hand side it can be seen that the spin-up time, i.e., the batch time required to reach a certain enrichment, scales with r_0^2/DA_0; the number of moles inside the centrifuge, m, scales with $r_0^2 l_0$. Therefore the production rate, $\dot{m} = \int \rho dV/\Delta t$, scales as $\rho D l_0 A_0$. For a given level of enrichment the production per unit time is only a function of centrifuge length and peripheral velocity (Cohen, 1951; Pratt, 1967).

Eq. (4) is solved in order to estimate product flow magnitude and composition of a 50/50 CH_4/CO_2 feed stream. We used Aspen Custom Modeller (ACM)—an equation oriented modelling package. The problem is set up as spatially axisymmetrically discretised along a uniform grid and time integration is performed with a fourth-order Runge–Kutta algorithm. Previous work has looked at a batch centrifuge (Auvil and Wilkinson, 1976; Golombok and Chewter, 2004). The current work extends the latter work and is used as a reference case for comparison with the countercurrent calculations. All calculations in this work are performed using an effective static fill pressure of 0.5 MPa and a fluid temperature of 293 K. This choice of conditions is influenced by a number of application factors. Reservoir gas pressures are typically on the order of 10–30 MPa but are reduced significantly at the well head typically being throttled to around 7 MPa. Previous gas centrifuge work has been based on low pressures because of the desublimation of UF_6. The limits for our study are therefore a feed pressure above atmospheric pressure but sufficiently low so that during centrifugation we do not reach dewpointing pressures (above 2.5 MPa). A feed pressure of 0.5 MPa fulfils this requirement. The results reported in this work are almost independent of pressure because the product ρD increases slightly for very high static fill pressures (> 7 MPa) which is academic as condensation will occur at this level anyway. In this study we used the value for the product $\rho D = 2.8 \times 10^{-5}$ kg/ms based on a calculation of known material properties for the gas mixture.

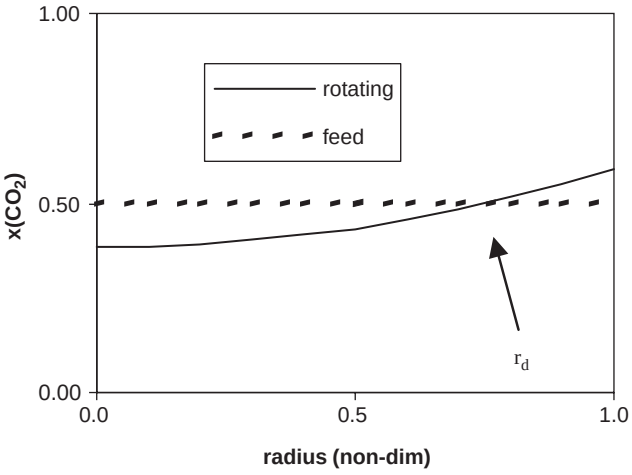

Fig. 2. Mole fraction of CO_2 as a function of non-dimensionalised radius in a 5 cm radius centrifuge spinning at 70 000 rpm. The arrow indicates the radial crossing point—the point where the imposed equilibrium concentration profile exceeds that of the feed.

In order to solve Eq. (4) the following boundary conditions have been applied:

$$\text{at } z^* = 0 \quad \text{and} \quad z^* = 1, \quad \text{for } 0 < r^* \leqslant 1: \ \frac{\partial x_1}{\partial z^*} = 0,$$

$$\text{at } r^* = 0, \quad \text{for } 0 \leqslant z^* \leqslant 1: \ \frac{\partial x_1}{\partial r^*} = 0,$$

$$\text{at } r^* = 1, \quad \text{for } 0 < z^* < 1: \ \frac{\partial x_1}{\partial r^*} = -2Ar_w^2 x_1(1-x_1),$$

which simply state symmetry around the axis and mass conservation at the walls.

Product flows are calculated by dividing the methane-enriched portion in the interior of the centrifuge by τ_{90}—the time required to reach 90% of the equilibrium steady-state enrichment (Golombok and Chewter, 2004), because reaching steady state would theoretically take an infinitely long time. The enriched fraction in the interior is everything inside the so-called radial crossing point, defined as the radius at which the composition is equal to the feed composition (Fig. 2). Bearing in mind the exponential pressure distribution inside the centrifuge (Eq. (1)) and the fact that the batch centrifuge is a closed system, it is easy to see that due to mass conservation the pressure in the centre of the centrifuge will be lower and the wall pressure will be higher than the static fill pressure (Golombok and Chewter, 2004).

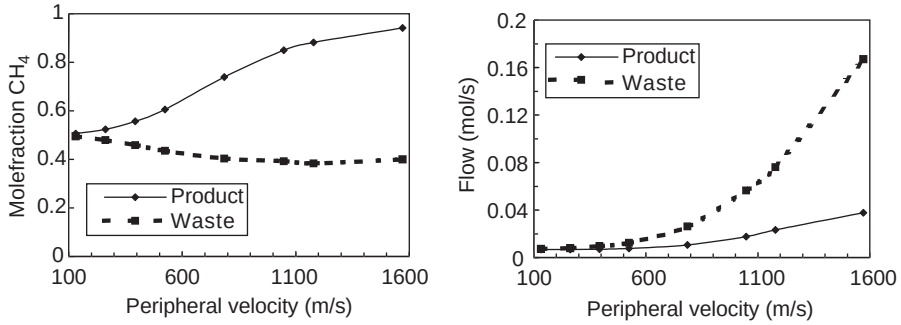

Fig. 3. (a) (left) and (b) (right). Mole fraction CH_4 and flows as a function of peripheral velocity for a 1 m long centrifuge.

The time τ_{90} is defined as the time required to get an average enrichment inside the product volume that is 90% of the steady-state enrichment. The time required for refilling, pressurising and spinning up the centrifuge is neglected in this model. Production scales linearly with length, thus results will be presented per unit length, i.e., for a 1 m long centrifuge. Fig. 3a and b show the mole fraction CH_4 and the product and waste flows as a function of peripheral velocity. The graphs are plotted for peripheral velocities up to 1600 m/s; however, with current commercial rotor technology it is not possible to have a higher velocity than 800 m/s. This is mainly due to material limitations (Cohen, 1951). Even at high velocities the production of a 1 m batch centrifuge is still very limited—on the order of kg/h—whereas what is required is 100s of ton/h—corresponding to 100s MMscf/d. The reason for this is that the separation process itself is dominated by diffusion, and since diffusion is very slow this results in a low production rate. The only way to augment the separation rate is to use the radial pressure gradient to dewpoint the heavier waste component as we have previously discussed (Cracknell and Golombok, 2004).

3. Continuous centrifuge

The batch process can be effectively accelerated by switching to a countercurrent process. Of course any practicable process has to be continuous and these may be divided up into cocurrent and countercurrent configurations (Cohen, 1951). The former is very similar to the batch process where the time coordinate is basically replaced by motion along the axial flow dimension. The flow is assumed laminarised by, for example, use of a channelled medium. This has previously been shown to decouple axial and radial turbulence—the radial flow must remain laminar of course so as not to spoil the centrifugal separation process. The countercurrent process is the one of interest because it is the most efficient and will form the emphasis in this section. It is well known from process engineering (and also convective heat transfer) that countercurrent processes with product (i.e., methane) and waste (i.e., contaminant) enriching streams flowing in opposite directions lead to the maximum radial concentration gradient and thus the most efficient separation mechanics.

3.1. Isotopic vs. natural gas centrifugation

The continuous countercurrent mode (as in many applications, e.g. heat exchangers) is the spatially most efficient operation. However when applied to the gas centrifuge, and as a result of the complicated coupling of extra terms, the formulation has a number of extra terms compared to the batch equation

$$\rho w \frac{\partial x_1}{\partial z} + \rho u \frac{\partial x_1}{\partial r} = \frac{D\rho}{r} \frac{\partial}{\partial r} \left(r \frac{\partial x_1}{\partial r} + 2(A_2 - A_1) r^2 x_1 (1 - x_1) \right) + D\rho \frac{\partial^2 x_1}{\partial z^2}, \quad (5)$$

where the symbols are as previously defined with the addition of z the axial direction and w the velocity component in that direction. In a continuous unit there is of course axial flow. In fact the replacement of $\partial/\partial t$ by $w\partial/\partial z$ is not strictly correct because now x_1 is z dependent, i.e., $x_1 = x_1(z)$, so a number of terms in the full equation need to be retained. In the original work available in the open literature, a number of mathematical issues in the handling of the equation are addressed (Cohen, 1951). This was necessary to deal with the restricted computing power available at the time. We now show that they are only valid for the heavy isotope separation case, and that they are not appropriate for natural gas processing. For example it was previously assumed that concentration gradients $\partial x_1/\partial r$ and $\partial x_1/\partial z$ are all small—this is not true for the methane/CO_2 centrifuge due to the boundary conditions and the spatial enrichment gradient that is imposed on a single unit. At any rate, advances in computing power mean that the full Eq. (5) can be handled—not a subject which appears to have been tackled—in the open literature at any rate.

The analytically based derivation of Cohen used simplifications of a number of parameters. The most important is the separation factor—usually defined by analogy with distilla-

tion for the batch case as the ratio of concentrations at the wall ($r = R$) divided by that at the centre (Olander, 1981):

$$S = \frac{x_1(0)/x_2(0)}{x_1(R)/x_2(R)}. \tag{6}$$

In all previous literature analyses this parameter is assumed to be close to 1. Those comparisons were aimed at deriving the separative power. This assumes that the centrifuge can separate components to provide a given product and waste stream composition, and the separative power gives the corresponding flow rate at which these separations can be achieved. Cohen showed that the separative power has a maximum value of

$$\delta U_{\max} = \frac{Dp}{R_g T}\left[(A_2 - A_1)R^2\right]^2 \frac{\pi L}{2}, \tag{7a}$$

where in addition to previously defined symbols, L is the length of the centrifuge. This separative power is a combination of quantity and quality for the flow and achieved separation. It is effectively the separation factor S in Eq. (6) above, combined with the flow at optimum internal flow conditions. The actual separation that can be achieved is given by

$$\delta U = \varepsilon \delta U_{\max}, \tag{7b}$$

where the factor ε is a function of the geometric configuration used and depends on the process flow and the number of "poles" in the system, i.e., the number of inlets and outlets. For example, a single feed inlet, product outlet and waste outlet constitutes a 3-pole system.

The assumptions used in deriving this term rested on the quantitative simplifications from assuming small concentration gradients as discussed earlier (Cohen, 1951). Crucial to the development of Eq. (7b) is the assumption that the elementary (unit) separation factor defined in Eq. (6) is only very slightly greater than 1. This is in contrast where $S \gg 1$. At various points in the derivation for the separation this assumption of "very small" $S-1$ is explicitly stated in order to simplify various sequential element balances in a cascade.

The difference between the molecular weights and the consequences it has for the analysis of the problem is the starting point for our analysis. We can compare the separation factor for isotopes and for natural gas in an experimentally realistic centrifuge. From our own experimental program (to be reported separately) it is clear that realistic material and mechanical process parameters for a centrifuge are in the range 32 000–100 000 rpm with rotor radii of 7–9 cm. Currently we can continuously centrifuge at 32 000 rpm with $R = 8.9$ cm. The limits are set by the rotor material tensile strength which limits the maximum speed at the periphery of the rotor—and also the sliding speed of the rotating seal. This purchasable technology is already more than a decade old and so we feel justified in using the upper limits of these ranges. Table 1 shows the parameters for the experimentally attainable configurations for both UF_6 and CH_4/CO_2. Notice that the separation factor is only nearly 1 for the lower speed isotope case. Yet this near unitary assumption is the basis for the extensive analysis and subsequent cascade requirements which have been carried out in the literature, i.e., the previously used assumptions for the countercurrent centrifuge are not correct. In our previous work we concentrated on the assumptions made in simplifying the countercurrent centrifuge equation. In a later account of the derivation of the separative power (Pratt, 1967), one finds this assumption of a near-unitary separation factor entering at a number of points into the derivation of the mass transport, resulting in separative power and the associated cascade configuration. Our main conclusion is that the assumptions used are thus not valid for the current state of technology and also not for the separation of natural gas components. For this reason we have re-examined the countercurrent centrifuge and rederive the associated equations without any of the simplifying assumptions which were only applicable to isotopes. Many of these simplifying assumptions date from a time when it was not possible to handle the full dynamic equations by numerical models. Although computer simulations have been able to do this for some time now, there has not been any report on addressing these issues—probably mainly because with two exceptions, all work has been concerned with isotopes. To the best of our knowledge no one has ever pointed out before that this underlying assumption is not valid when it comes to considering lighter molecular weight components such as those found in natural gas.

Table 1
Comparison of separation factors for classical isotope and natural gas contaminant separations in a gas centrifuge

Speed (rpm)	Rotor radius (cm)	Separated material	S—separation factor
32 000	8.9	$^{235}UF_6/^{238}UF_6$	1.06
32 000	8.9	CH_4/CO_2	1.7
100 000	7	$^{235}UF_6/^{238}UF_6$	1.4
100 000	7	CH_4/CO_2	27.4

Since the derivation of unit separative power (Eq. (3)) seems to rest explicitly at several places on the $S \approx 1$, small product to feed ratios and also small concentration gradient assumptions, which we have demonstrated to not be valid for natural gas, it seems to us worth the effort that the model should at least solve the countercurrent equations for the centrifuge explicitly, rather than simply estimating the separations by using Eq. (3) which we have now demonstrated to rest on inapplicable premises for the natural gas case.

3.2. Countercurrent model

In order to perform numerical calculations on the countercurrent centrifuge, we non-dimensionalise the velocity field with physical parameters. Let us therefore first outline the working principle of the countercurrent centrifuge. The basics are the same as previously reported: a high-speed rotating hollow cylinder, filled with gas and a mole frac-

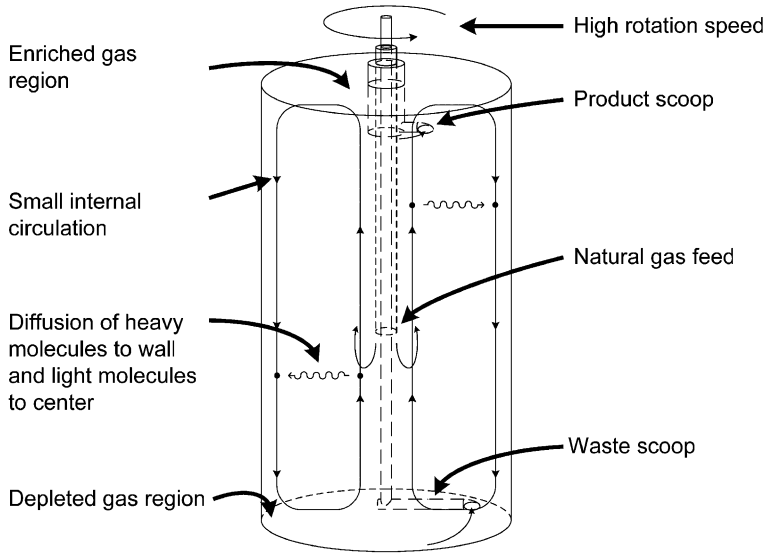

Fig. 4. Schematic of countercurrent centrifuge.

tion gradient over the radius (Fig. 1). Now a small internal circulation is imposed, either thermodynamically by heating at the bottom and cooling at the top or mechanically. This recirculating flux is varied in order to find the optimum performance—we shall see below that it is related to the Peclet number. It is also obvious that it cannot be much larger than the feed rate because this will slow down the process. Due to this circulation the gas is moving upwards at the centre and downwards at the outer wall. The upward moving stream is continuously enriched in the lighter element due to diffusion along the concentration gradient resulting from the imposed centrifugal field. In the downward streams the opposite occurs. A gas feed is added at the point on the axis where the feed composition is equal to the local composition. This is required to prevent mixing at the feed point. At the top and bottom of the centrifuge the product and waste are collected by scoops. This working principle of the countercurrent centrifuge is shown schematically in Fig. 4. Note that the radial flux can occur via the porous channelled medium which we have previously introduced in order to suppress turbulence which would disable the centrifugal separation (Brouwers, 1978a).

3.3. Bulk flow field

Fig. 5 represents the flow field in the bulk volume of the centrifuge. As indicated in Fig. 4 the motion is upwards near the middle of the centrifuge and downwards near the wall. There is a requirement of course that for pure recirculation (i.e., when there is no material added or withdrawn) then along any radial line the net upward mass flow must balance that downwards (i.e., the fluxes integrated across the axial cross-sectional areas).

Since the velocity field inside the centrifuge is mainly axial we non-dimensionalise the axial mole flux with respect to the magnitude of the upward mass flow. We de-

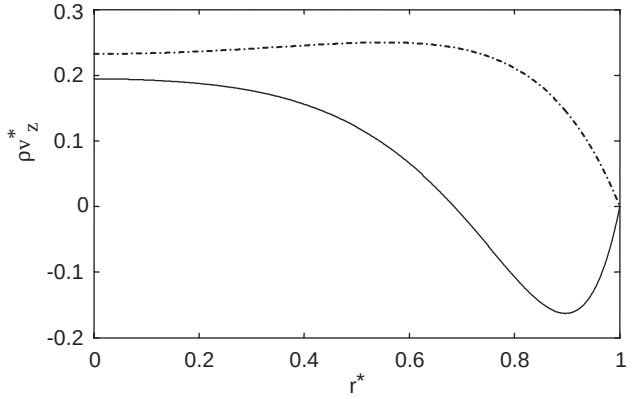

Fig. 5. Countercurrent flow profiles in a centrifuge. Solid line: circulating flow, $F=P=W=0$; dotted line: flow above feedpoint, $\phi_{mc}=0$, $P/F=1$.

fine this countercurrent mass flow (kmol/s) ϕ_{mc} as the total mass flow of the internal circulating stream flowing upward in the centre of the centrifuge ϕ_{mc} from $r=0$ to $r=r_1$, where r_1 is the radius $0<r_1<r_0$ at which the axial velocity $v_z=0$. Due to mass conservation this mass flow is equal to the mass flowing down in the outer radii of the centrifuge. (Previously the value of the summed axial flow is taken as a scaling parameter (Cohen, 1951)—this is twice our own non-dimensionalising factor.)

$$\phi_{mc}=2\pi\int_0^{r_1}\rho v_z r\,\mathrm{d}r. \tag{8}$$

This then leads to our definition of the dimensionless mole flux $(\rho v_i)^*$ profile in direction i which for the axial direction leads to

$$(\rho v_z)^*=\frac{r_0^2}{\phi_{mc}}\rho v_z \tag{9}$$

and for the radial direction results in

$$(\rho v_r)^* = \frac{r_0 l_0}{\phi_{mc}} \rho v_r. \tag{10}$$

The definition of Eqs. (9) and (10) requires that the integral of $(\rho v_z)^*$ from 0 to r_1 is equal to 1. Since this is not the case for the velocity profiles used in this study, it is required that the left-hand sides of Eqs. (9) and (10) are multiplied by a normalisation factor, β. This normalisation factor can be calculated by inserting Eq. (9) into Eq. (8), adding the desired velocity profile and solving the resulting equation for $\phi_{mc} = 1$. (For the velocity profiles discussed here, the normalisation factor $\beta = 5.8$.)

Because we need to calculate flows in both the z and r directions, we make use of the stream function—a scalar function Ψ which fully describes a 2D flow field. In this case the flow field is axisymmetric and therefore 2D. The axial and radial velocity field can be calculated by taking respectively the radial and axial derivative of the stream function, i.e., $(\rho \mathbf{v})^* = \nabla(\rho\Psi)$.

In order to calculate the dimensionless velocity field or stream function the full Navier–Stokes equations have to be solved. A full direct numerical simulation (DNS) is not possible due to the high Reynolds numbers involved. For example, simple developed axisymmetric pipe flow can be modelled by DNS for Reynolds numbers up to 15 000. In that case the largest computer in the Netherlands requires 3 months calculation time in order to get sufficient information on random fluctuations. Note that in our case, because of higher pressure, the Reynolds numbers are larger than for the isotope case—and required computer power increases exponentially with Reynolds number. Because of this complexity, an approximate solution will be used (Brouwers, 1978b):

$$\rho\Psi = \mathrm{e}^{-x}(1 - \mathrm{e}^{-x} - x\mathrm{e}^{-x}), \tag{11}$$

where $x = A\psi(1 - r^{*2})$ and $A\psi = v_w^2 \bar{M}/(2RT)$.

Eq. (11) is the analytical solution for the bulk flow in case the countercurrent stream is generated by a linear axial temperature gradient on the wall. This solution is an approximation of the solution for a stream generated by heating and cooling bottom and top end-caps (Brouwers, 1978a), which is the accepted method for convectively ensuring recirculation in the centrifuge. This is of course an arbitrary solution, but has been shown previously to be of validity for modelling countercurrent flow in a centrifuge.

3.4. Flow field at ends

Since there is no z-dependent part in Eq. (11) it actually describes an infinitely long centrifuge. In an actual centrifuge with a finite length the flow reverses at the top and bottom in very thin boundary layers, the so-called Ekman layers (Brouwers, 1978a). To avoid complexity these layers are modelled using a very steep exponential function; mass conservation is preserved:

$$\rho\Psi = \mathrm{e}^{-x}(1 - \mathrm{e}^{-x} - x\mathrm{e}^{-x})(1 - \mathrm{e}^{-z^*/\lambda}) \times (1 - \mathrm{e}^{(-1-z^*)/\lambda}), \tag{12}$$

where λ is the dimensionless reversion layer thickness.

3.5. Input and output flow fields

So far only the flow field resulting from the countercurrent motion has been considered. The actual flow field also incorporates the flow induced by the feed stream and product and waste outlet. This flow can be described in a similar way as done for the circulating flow; however the non-dimensionalisation factor is now the feed flow rate F:

$$f_z(r^*, z^*) = \frac{r_0^2}{F}(\rho v_z)_{PW} \tag{13a}$$

and

$$f_r(r^*, z^*) = \frac{r_0 l_0}{F}(\rho v_r)_{PW}, \tag{13b}$$

where F is the feed flow rate (kmol/s) at the injection point $z^* = z_F^*$ and f_i the dimensionless mole flux profile of the feed/product/waste flow in direction i.

Normalisation factors may be required, depending on the mole flux profiles that are used. These can be incorporated in Eqs. (13a and b) in a similar way as described above. The dimensionless mole flux profiles, f_z and f_r, are calculated using analytical solutions by Brouwers (1978a,b). According to this work, the feed–product–waste flow is positive above the feed point and negative below it. This phenomenon is modelled by a continuous function with a finite gradient to stabilise the numerical simulations. The full feed–product–waste dimensionless mole flux profiles are

$$\begin{aligned} f_z(r^*, z^*) &= \frac{1}{2}\mathrm{e}^{-(1-r^{*2})}(1 - \mathrm{e}^{-(1-r^{*2})}) \\ &\quad \times \left[\Theta\left(\tanh\left(\frac{(z^* - z_F^*)}{\lambda_F}\right) + 1\right)\Big/ 2 \right. \\ &\quad \left. + (1 - \Theta)\left(\tanh\left(\frac{(z^* - z_F^*)}{\lambda_F}\right) - 1\right)\right], \end{aligned} \tag{14a}$$

$$f_r(r^*, z^*) = \frac{1}{r^*}\frac{((\tanh((z^* - z_F^*)/\lambda_F))^2 - 1)}{2\lambda_F} \times \left(\frac{1}{2}\mathrm{e}^{-(1-r^{*2})} - \frac{1}{4}\mathrm{e}^{-2(1-r^{*2})} - \frac{1}{4}\right). \tag{14b}$$

Similarly we can define the output product stream as

$$\begin{aligned} P &= 2\pi \int_0^{r_1} (\rho v_z)_{PW}|_{z^*=1} r \, \mathrm{d}r \\ &= 2\pi \int_0^1 \xi f_z|_{z^*=1} r^* \, \mathrm{d}r^*, \end{aligned} \tag{15a}$$

where ξ is the normalisation constant, calculated by

$$\xi_{\text{cal}} = \frac{1}{2\pi \int_0^1 \mathrm{e}^{-(1-r^{*2})}(1-\mathrm{e}^{-(1-r^{*2})})r^* \,\mathrm{d}r^*} \tag{15b}$$

which has a value of 1.6 for our study. P is the product flow rate and Θ is product/feed ratio. The total flow field is calculated by superposition of the countercurrent velocity field and the feed/product/waste velocity field:

$$\rho v_z = \frac{\phi_{mc}\beta_{\text{cal}}}{r_0^2}(\rho v_z)_0^*, \tag{16}$$

where

$$(\rho v_z)_0^* = \left((\rho v_z)^* + F_0 \frac{\xi}{\beta} f_z(r^*, z^*)\right) \tag{17}$$

and $F_0 = F/\phi_{mc}$. (The physical meaning of these parameters is discussed below.) Using the balancing procedure described in our previous work whereby the difference in component mass flow in and out of an axial section is equated to the radial induced flow through the corresponding annulus and considering stationary operation only, the convection–diffusion equation for the countercurrent centrifuge becomes in dimensionless form

$$\begin{aligned}\phi^* &\left[(\rho v_z)_0^* \frac{\partial x_1}{\partial z^*} + (\rho v_r)_0^* \frac{\partial x_1}{\partial r^*}\right] \\ &= \frac{1}{r^*}\frac{\partial}{\partial r^*}\left(r^* \frac{\partial x_1}{\partial r^*} + 2A_0 x_1(1-x_1)r^{*2}\right) \\ &\quad + \alpha^2 \frac{\partial^2 x_1}{\partial z^{*2}}.\end{aligned} \tag{18}$$

The significance of ϕ^*, A_0 and α are now discussed.

3.6. Controllable parameters

Based on the non-dimensionalisation to reach Eq. (18) the three independent dimensionless numbers can be identified in this equation—ϕ^*, A_0 and α—and are defined from the derivations as

$$\phi^* = \frac{\phi_{mc}}{\rho D l_c} \approx \frac{r_0^2 v}{D l_c}. \tag{19}$$

This represents the non-dimensionalised recirculating flow defined above. We have in fact nondimensionalised the inertial flow with the diffusive flow—when simplified, this parameter is the same as the more familiar Peclet number *Pe*. Physically this means that the small internal circulation introduced above is on the order of 10^{-5} kmol/s. ϕ^* is a variable parameter—we shall see that it is the only parameter with an optimal value for separation. Working back through Eqs. (19) and (8) we arrive at the value of the order of 10^{-5} kmol/s. The optimum value of near-unitary *Pe* number is also explained physically by the fact that the inertial processes must not dominate the diffusive process otherwise poor separation will be achieved:

$$A_0 = A r_0^2. \tag{20}$$

This represents the non-dimensionalised centrifuge instrument parameter and contains the interaction between the gaseous material (the molecular weight thus) and the mechanical parameters of the centrifuge, namely the radius and the rotational speed:

$$\alpha = \frac{r_0}{l_0}. \tag{21}$$

This number is the aspect ratio of the centrifuge. These numbers fully determine the outcome of the equation and are a function of the design parameters ϕ_{mc}, l_c, v_w and the radius/length ratio of the centrifuge. With the addition of feed, product and waste flows, two more variables enter the equation, namely F_0 the feed rate non-dimensionalised against the recirculating flow

$$F_0 = \frac{F}{\phi_{mc}} \tag{22}$$

and Θ defined by the product flow to feed flow ratio

$$\Theta = \frac{P}{F}. \tag{23}$$

So in total 5 independent variables (Eqs. (19–23)) can be identified in the convection–diffusion equation of a countercurrent centrifuge.

4. Results

The influence of these 5 variables is investigated using numerical simulation of the convection–diffusion equation. As in our previous work, Aspen Custom Modeler (ACM) is used to solve Eq. (18). Boundary conditions of the countercurrent centrifuge are similar to those of the batch centrifuge, except for the feed point. At this point, located somewhere on the axis, the boundary condition is that of a fixed composition instead of mass conservation. The exact location of the feed point on the axis cannot be chosen arbitrarily; in order to prevent mixing the feed point has to be chosen such that the feed composition is equal to the local composition. This process of selecting the feed point location is dependent on the solution of the convection–diffusion equation, which in turn is dependent on the feed point location. Therefore, the location of the feed point has to be determined iteratively. Also, the feed point location is dependent on the 5 independent variables, i.e., a change in one of these variables inevitably leads to a change in the feed point location. In real life application this does not lead to any problems: countercurrent centrifuges are meant to be operated in steady–state conditions. In case of the simulations mentioned above the feed point matching adds more complexity to the numerical solving process.

Table 2
Controllable parameter values expressed in the non-dimensionalised form corresponding to the standard case used in the simulations

ϕ^*	2.73
A_0	1.4
α	0.06
F_0	0.92
Θ	0.4

Using ACM the convection–diffusion equation is solved for a standard case (see Table 2). This standard case is defined using existing knowledge and consideration of mechanical properties. It is known that the peripheral velocity of the centrifuge should be as large as possible and due to mechanical limitations this can be anywhere from 350 to 800 m/s. This is based on commercially available ultracentrifuges which we are developing for an experimental program. An example is a commercial centrifuge manufactured by Beckman Coulter and modified by us, which rotates at 100 000 rpm and has a diameter of 14 cm with a corresponding peripheral velocity of 750 m/s (Brouwers, 1978b). A quite moderate value is thus 500 m/s which is selected for the standard case. Together with $\Delta M = 28$ g/mol for CH_4/CO_2 mixtures this leads to $A = 1.4$ for ambient temperature conditions. The radius/length, α, ratio depends on the required axial stiffness and can range from 0.02 to 0.2 or even larger. Previous research on isotope centrifuges indicates that α should be as small as possible (Los, 1963; Brouwers, 1976). Therefore a value of $\alpha = 0.06$ is selected for the standard case. For the product/feed ratio also a moderate value is selected on the bases of literature: $\Theta = 0.4$; any value from 0 to 1 can of course be selected. The last two variables, F_0 and ϕ^*, depend on feed composition and required enrichment. Again a feed mixture of 50 mol% CH_4 and 50 mol% CO_2 is considered. The product stream should have a composition of 80 mol% CH_4. (This leads to a feed flow of 3×10^{-3} mol/s.) The 5 independent variables are varied one at a time, i.e., 4 variables are kept at their value for the standard case. Results of these simulations are shown in Fig. 6.

The ranges of the above figures are chosen such that they comply with realistic conditions. The lines drawn in the figures are trend lines. Fig. 6(d) and (e) show the most important and obvious trend: an increase in the feed flow rate results in a decrease of the enrichment. It is concluded from Fig. 6 that there is an optimal ϕ^*-value which leads to a maximum enrichment at a given flow rate. This means that ϕ^* cannot be chosen arbitrarily; only one ϕ^* gives the maximum efficiency.

An increase in A results in a strong increase in enrichment. This works two ways: for a certain enrichment level an increase in A results in an increased flow rate, i.e., higher production levels are possible for higher values of A. Thus performance increases with increasing peripheral velocities and molecular weight differences—this is in line with the earlier presented results of the batch centrifuge (Golombok and Chewter, 2004). Varying the radius/length ratio has a large influence on the enrichment; the smaller this ratio, the higher the enrichment. The dynamic properties of the centrifuge limit its length. e.g. the bending stiffness, a function of the radius/length ratio, should be high enough to withstand the vibration forces that occur due to the high-speed rotation (Groth and Beyerle, 1961).

The product/feed ratio has no real influence on performance. It can be used to set the balance between enrichment and depletion of product and waste, i.e., a lower product/feed ratio results in a higher enrichment of the product and a lower depletion of the waste. Using these results and considering material limitations an optimised centrifuge configuration is calculated for the 50/50 CH_4/CO_2 case. Commercial available centrifuge cores can rotate with a maximal peripheral velocity of 750 m/s. The minimum value of the radius/length ratio is 0.02 for these units. Setting the product/feed ratio at 0.3 results together with the above values to a maximum flow of 8×10^{-5} kmol/s for an enrichment from $x_{F,CH_4} = 0.5$ to $x_{P,CH_4} = 0.7$ in a 5 m long unit. The optimal value for ϕ^* is in this case 2.8. Although significantly enhanced, the available throughput still falls far short of the desired level for natural gas separation.

5. Conclusions

1. Centrifugation of a contaminated gas mixture into a gaseous product (CH_4) stream and gaseous waste (CO_2) stream cannot be carried out fast enough to perform the separation in one or a small number of units at the required commercial rates (100s MMscf/d, i.e., on the order of 100 tons per hour). The schemes using large numbers of centrifuges in cascades are not economically feasible for natural gas.
2. Centrifugal separation of natural gas has a significant number of component and process differences from the separation of isotopes. The lighter molecular weights and large product and waste molecular weight differences lead to a non-unity separation factor. The correct analysis for the non-unitary values of separation factor has been carried out.
3. The enhancement due to countercurrent centrifugation compared to the batch process is still not sufficient to make the gas–gas process interesting.
4. All calculations in this work were based on the example of a 50/50 CH_4/CO_2 mixture. In real applications, contaminated gas fields extend from the currently treatable limit of ca. 10% CO_2 to up to 70% CO_2. At the lower level of contamination the relatively smaller concentration gradient will increase separation times. At higher concentrations the effect of condensation on the centrifuge will become much more important and since this is a fast process, the separation will occur more quickly.

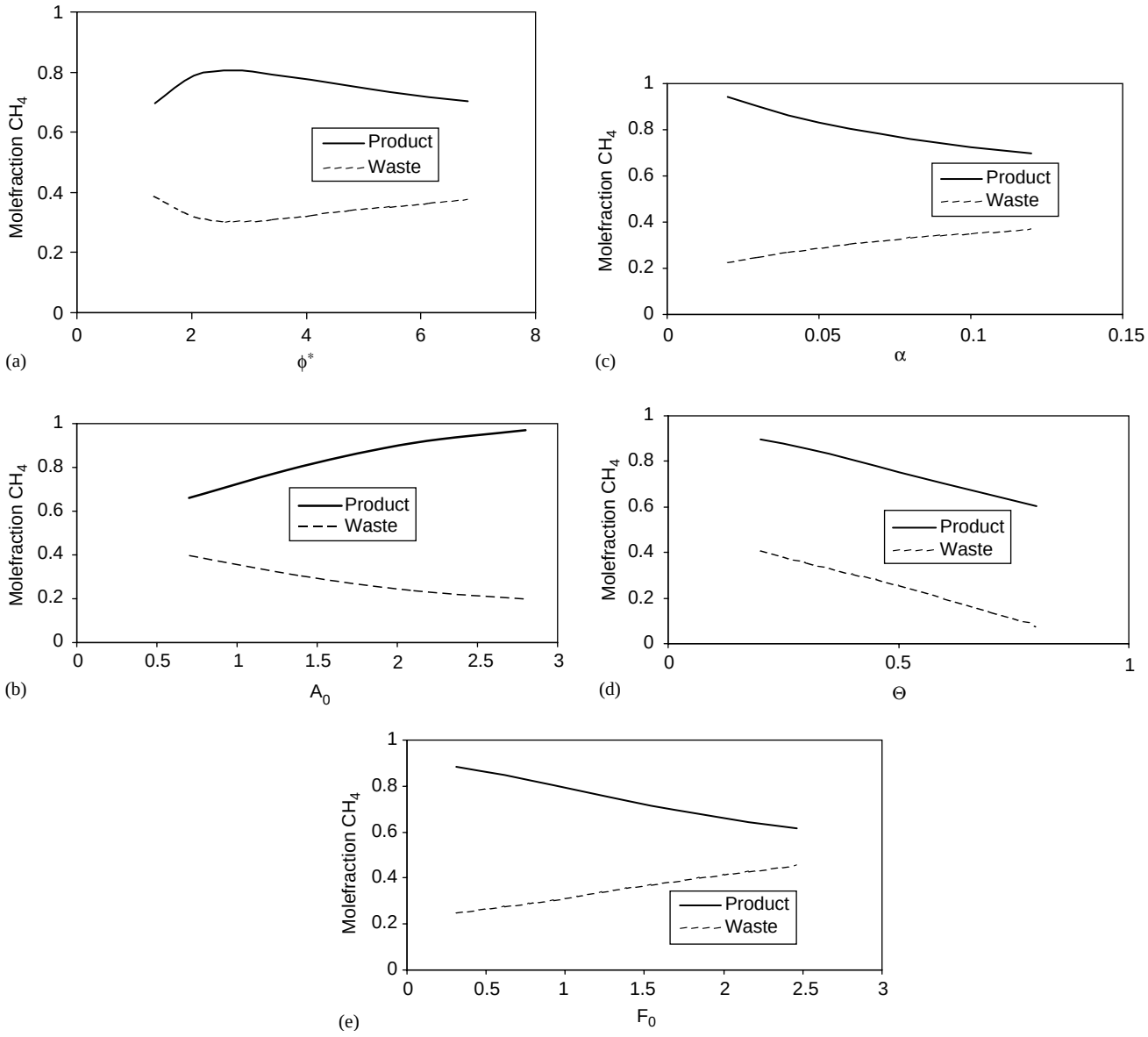

Fig. 6. Concentration (mole fraction $CH_4 x_{CH_4}$ in product and waste streams as a function of the 5 independent variables, x_{CH_4} vs (a) ϕ^*—normalised convective recirculation/diffusive ratio, (b) A_0—centrifuge operating parameters, (c) α—aspect ratio, (d) Θ—product–feed ratio and (e) F_0—feed/recirculation ratio.

5. Increasing the separation rates requires boosting the mass transfer rates and spatial separation rate of product and waste. Using the radial pressure gradient to cause phase separation is one way forward and this is the focus of our current modelling and experimental efforts. This would require some cooling: for example for the 50/50 CH_4/CO_2 mixture analysed in this study, the temperature needs to be below $-10°C$ so that compression will cross the dewpointing curve. However many of the fields have higher levels of contamination—for a 70% CO_2 field, this temperature is only 9°C. Cooling the gas is in itself no problem, as the high reservoir pressure make expansion cooling a straightforward procedure.
6. In the above study we were concerned with removing a single contaminant from a pure natural gas stream. In reality of course, gas streams contain multiple components of different molecular weights. The only difference this would make is the complexity of the equations. In the above treatment all equations are binary—there is one component and the other one is complementary. An additional component simply doubles the calculation time. For transparency, and in order not to obscure the essential physics, we confined our calculation to the binary case in order to home in on the essential problem; however the result is equally valid for multiple components.

Notation

A	centrifuge instrument parameter, $1/m^2$
A_0	dimensionless centrifuge instrument parameter
D	diffusion coefficient, m^2/s
f_i	dimensionless feed–product–waste mole flux profile in direction i
F	feed flow rate, kmol/s
F_0	feed flow/recirculating flow ratio
l_0	centrifuge length, m
L	centrifuge length, m
M	molar weight, kg/kmol
p	pressure, Pa
p_0	pressure at $r = 0$, Pa
p_{wall}	pressure at wall, Pa
P	product flow rate, kmol/s
r	radial coordinate, m
r^*	dimensionless radial coordinate
r_0	centrifuge radius, m
R	wall radius, m
R_g	universal gas constant, J/kmol/K
S	separation factor
t	time, s
T	temperature, K
u	radial mixture velocity, m/s
v_0	peripheral velocity, m/s
v_i	gas mixture velocity in direction i, m/s
w	axial mixture velocity, m/s
W	waste flow rate, kmol/s
x	mole fraction
z	axial coordinate, m
z^*	dimensionless axial coordinate
z_F^*	dimensionless axial coordinate of feed point

Greek letters

α	aspect ratio of the centrifuge
β	normalisation factor for countercurrent flow
δU	separative power, kmol
ζ	normalisation factor for feed–product–waste flow
Θ	product/feed ratio
λ	boundary layer thickness parameter
λ_F	product/waste transition layer thickness parameter
ρ	gas mixture density, $kmol/m^3$
(ρv_i)	dimensionless countercurrent mole flux profile in direction i
(ρv_j)	dimensionless mole flux profile in direction i
$\tau 90$	time to reach 90% of steady-state enrichment, s
ϕ	dimensionless recirculating flow
ϕ_{mc}	countercurrent flow rate, kmol/s
Ψ	dimensionless stream function
Ω	angular velocity, rad/s

References

Astarita, G., Savage, D.W., Bisio, A., 1983. Gas Treating with Chemical Solvents. Wiley, New York.

Auvil, S.R., Wilkinson, B.W., 1976. The steady and unsteady state analysis of a simple gas centrifuge. A.I.Ch.E. Journal 22 (3), 564–568.

Beams, J.W., Skarstrom, C., 1939. The concentration of isotopes by the evaporative centrifuge method. Physical Review 266, 56.

Brouwers, J.J.H., 1976. On the motion of a compressible fluid in a rotating cylinder. Ph.D. Thesis, Twente University of Technology, Enschede, The Netherlands.

Brouwers, J.J.H., 1978a. On compressible flow in a gas centrifuge and its effect on the maximum separative power. Nuclear Technology 39, 311–322.

Brouwers, J.J.H., 1978b. On compressible flow in a rotating cylinder. Journal of Engineering Mathematics 12 (3), 265–285.

Cohen, K.P., 1951. The Theory of Isotope Separation as Applied to the Large-Scale Production of U-235. McGraw-Hill, New York.

Cracknell, R., Golombok, M., 2004. Monte Carlo simulations of centrifugal gas separation. Molecular Simulations 30 (8), 501.

Golombok, M., Chewter, L., 2004. Centrifugal separation for cleaning well gas streams. Industrial and Engineering Chemistry Research Design 43 (7), 1734.

Golombok, M., Morley, C., 2004. Thermodynamic factors governing centrifugal separation of natural gas. Chemical and Engineering Research Design 82 (A4), 513.

Groth, W., Beyerle, K., 1961. Gas centrifuges. In: London, H. (Ed.), Separation of Isotopes. George Newnes, London.

Kohl, A.L., Nielsen, R.B., 1997. Gas Purification. Gulf, Houston.

Los, J., 1963. De scheiding van zware isotopen in een centrifugaal veld. Ph.D. Thesis, Leiden University, Leiden, The Netherlands.

Maddox, R.N., Morgan, D.J., 1998. Gas conditioning and processing. Vol. 4 : Gas Treating and Sulfur Recovery. Campbell Petroleum Series, Norman, USA.

Olander, D.R. The theory of uranium enrichment by the gas centrifuge. Progress in Nuclear Energy 1981, 8(1), 1.

Pratt, H.R.C., 1967. Countercurrent Separation Processes. Elsevier, Amsterdam.

Williams, L. O., 1980. Application of centrifugal separation to the production of hydrogen from coal. Applied Energy 6, 63.